Search for an H-Dibaryon with a Mass near $2m_\Lambda$ in $\Upsilon(1S)$ and $\Upsilon(2S)$ Decays

B. H. Kim,[46] S. L. Olsen,[46] I. Adachi,[10] H. Aihara,[52] D. M. Asner,[43] V. Aulchenko,[2] A. Bay,[25] K. Belous,[16] B. Bhuyan,[12] G. Bonvicini,[56] A. Bozek,[38] M. Bračko,[27,19] T. E. Browder,[9] V. Chekelian,[28] A. Chen,[35] B. G. Cheon,[8] K. Chilikin,[18] R. Chistov,[18] I.-S. Cho,[58] K. Cho,[22] V. Chobanova,[28] S.-K. Choi,[7] Y. Choi,[47] D. Cinabro,[56] J. Dalseno,[28,49] Z. Doležal,[3] S. Eidelman,[2] D. Epifanov,[2] S. Esen,[4] H. Farhat,[56] J. E. Fast,[43] V. Gaur,[48] S. Ganguly,[56] R. Gillard,[56] Y. M. Goh,[8] K. Hayasaka,[33] H. Hayashii,[34] Y. Hoshi,[50] W.-S. Hou,[37] Y. B. Hsiung,[37] H. J. Hyun,[24] K. Inami,[32] A. Ishikawa,[51] R. Itoh,[10] Y. Iwasaki,[10] T. Julius,[29] D. H. Kah,[24] J. H. Kang,[58] P. Kapusta,[38] E. Kato,[51] H. Kichimi,[10] H. J. Kim,[24] H. O. Kim,[24] J. H. Kim,[22] K. T. Kim,[23] M. J. Kim,[24] S. K. Kim,[46] Y. J. Kim,[22] K. Kinoshita,[4] J. Klucar,[19] B. R. Ko,[23] P. Kodyš,[3] S. Korpar,[27,19] R. T. Kouzes,[43] P. Križan,[26,19] P. Krokovny,[2] T. Kumita,[54] A. Kuzmin,[2] Y.-J. Kwon,[58] J. S. Lange,[5] S.-H. Lee,[23] J. Li,[46] X. Li,[46] Y. Li,[55] J. Libby,[13] D. Liventsev,[10] D. Matvienko,[2] K. Miyabayashi,[34] H. Miyata,[40] R. Mizuk,[18,30] G. B. Mohanty,[48] A. Moll,[28,49] N. Muramatsu,[45] R. Mussa,[17] E. Nakano,[42] M. Nakao,[10] E. Nedelkovska,[28] C. Ng,[52] N. K. Nisar,[48] S. Nishida,[10] K. Nishimura,[9] T. Ohshima,[32] S. Okuno,[20] P. Pakhlov,[18,30] G. Pakhlova,[18] H. Park,[24] H. K. Park,[24] M. Peters,[9] M. Petrič,[19] L. E. Piilonen,[55] M. Ritter,[28] S. Ryu,[46] H. Sahoo,[9] Y. Sakai,[10] S. Sandilya,[48] T. Sanuki,[51] V. Savinov,[44] O. Schneider,[25] G. Schnell,[1,11] C. Schwanda,[15] A. J. Schwartz,[4] D. Semmler,[5] K. Senyo,[57] O. Seon,[32] M. E. Sevior,[29] M. Shapkin,[16] V. Shebalin,[2] C. P. Shen,[32] T.-A. Shibata,[53] J.-G. Shiu,[37] B. Shwartz,[2] F. Simon,[28,49] P. Smerkol,[19] Y.-S. Sohn,[58] A. Sokolov,[16] E. Solovieva,[18] S. Stanič,[41] M. Starič,[19] M. Sumihama,[6] T. Sumiyoshi,[54] U. Tamponi,[17] K. Tanida,[46] G. Tatishvili,[43] Y. Teramoto,[42] K. Trabelsi,[10] M. Uchida,[53] S. Uehara,[10] T. Uglov,[18,31] Y. Unno,[8] S. Uno,[10] Y. Usov,[2] C. Van Hulse,[1] G. Varner,[9] V. Vorobyev,[2] M. N. Wagner,[5] C. H. Wang,[36] P. Wang,[14] Y. Watanabe,[20] K. M. Williams,[55] E. Won,[23] Y. Yamashita,[39] V. Zhilich,[2] and A. Zupanc[21]

(Belle Collaboration)

[1]*University of the Basque Country UPV/EHU, 48080 Bilbao*
[2]*Budker Institute of Nuclear Physics SB RAS and Novosibirsk State University, Novosibirsk 630090*
[3]*Faculty of Mathematics and Physics, Charles University, 121 16 Prague*
[4]*University of Cincinnati, Cincinnati, Ohio 45221*
[5]*Justus-Liebig-Universität Gießen, 35392 Gießen*
[6]*Gifu University, Gifu 501-1193*
[7]*Gyeongsang National University, Chinju 660-701*
[8]*Hanyang University, Seoul 133-791*
[9]*University of Hawaii, Honolulu, Hawaii 96822*
[10]*High Energy Accelerator Research Organization (KEK), Tsukuba 305-0801*
[11]*Ikerbasque, 48011 Bilbao*
[12]*Indian Institute of Technology Guwahati, Assam 781039*
[13]*Indian Institute of Technology Madras, Chennai 600036*
[14]*Institute of High Energy Physics, Chinese Academy of Sciences, Beijing 100049*
[15]*Institute of High Energy Physics, Vienna 1050*
[16]*Institute for High Energy Physics, Protvino 142281*
[17]*INFN-Sezione di Torino, 10125 Torino*
[18]*Institute for Theoretical and Experimental Physics, Moscow 117218*
[19]*J. Stefan Institute, 1000 Ljubljana*
[20]*Kanagawa University, Yokohama 221-8686*
[21]*Institut für Experimentelle Kernphysik, Karlsruher Institut für Technologie, 76131 Karlsruhe*
[22]*Korea Institute of Science and Technology Information, Daejeon 305-806*
[23]*Korea University, Seoul 136-713*
[24]*Kyungpook National University, Daegu 702-701*
[25]*École Polytechnique Fédérale de Lausanne (EPFL), Lausanne 1015*
[26]*Faculty of Mathematics and Physics, University of Ljubljana, 1000 Ljubljana*
[27]*University of Maribor, 2000 Maribor*
[28]*Max-Planck-Institut für Physik, 80805 München*
[29]*School of Physics, University of Melbourne, Victoria 3010*
[30]*Moscow Physical Engineering Institute, Moscow 115409*
[31]*Moscow Institute of Physics and Technology, Moscow Region 141700*
[32]*Graduate School of Science, Nagoya University, Nagoya 464-8602*
[33]*Kobayashi-Maskawa Institute, Nagoya University, Nagoya 464-8602*

[34]Nara Women's University, Nara 630-8506
[35]National Central University, Chung-li 32054
[36]National United University, Miao Li 36003
[37]Department of Physics, National Taiwan University, Taipei 10617
[38]H. Niewodniczanski Institute of Nuclear Physics, Krakow 31-342
[39]Nippon Dental University, Niigata 951-8580
[40]Niigata University, Niigata 950-2181
[41]University of Nova Gorica, 5000 Nova Gorica
[42]Osaka City University, Osaka 558-8585
[43]Pacific Northwest National Laboratory, Richland, Washington 99352
[44]University of Pittsburgh, Pittsburgh, Pennsylvania 15260
[45]Research Center for Electron Photon Science, Tohoku University, Sendai 980-8578
[46]Seoul National University, Seoul 151-742
[47]Sungkyunkwan University, Suwon 440-746
[48]Tata Institute of Fundamental Research, Mumbai 400005
[49]Excellence Cluster Universe, Technische Universität München, 85748 Garching
[50]Tohoku Gakuin University, Tagajo 985-8537
[51]Tohoku University, Sendai 980-8578
[52]Department of Physics, University of Tokyo, Tokyo 113-0033
[53]Tokyo Institute of Technology, Tokyo 152-8550
[54]Tokyo Metropolitan University, Tokyo 192-0397
[55]CNP, Virginia Polytechnic Institute and State University, Blacksburg, Virginia 24061
[56]Wayne State University, Detroit, Michigan 48202
[57]Yamagata University, Yamagata 990-8560
[58]Yonsei University, Seoul 120-749

(Received 16 February 2013; revised manuscript received 3 May 2013; published 31 May 2013)

We report the results of a high-statistics search for H dibaryon production in inclusive $\Upsilon(1S)$ and $\Upsilon(2S)$ decays. No indication of an H dibaryon with a mass near the $M_H = 2m_\Lambda$ threshold is seen in either the $H \to \Lambda p\pi^-$ or $\Lambda\Lambda$ decay channels and 90% confidence level branching-fraction upper limits are set that are between one and two orders of magnitude below the measured branching fractions for inclusive $\Upsilon(1S)$ and $\Upsilon(2S)$ decays to antideuterons. Since $\Upsilon(1S, 2S)$ decays produce flavor-$SU(3)$-symmetric final states, these results put stringent constraints on H dibaryon properties. The results are based on analyses of 102 million $\Upsilon(1S)$ and 158 million $\Upsilon(2S)$ events collected with the Belle detector at the KEKB e^+e^- collider.

DOI: 10.1103/PhysRevLett.110.222002 PACS numbers: 14.20.Pt, 12.39.Ba, 13.85.Rm

In 1977, Jaffe predicted the existence of a doubly strange, six-quark structure ($uuddss$) with quantum numbers $I = 0$ and $J^P = 0^+$ and a mass that is $\simeq 80$ MeV below the $2m_\Lambda$ threshold, which he called the H dibaryon [1]. An $S = -2$, baryon-number $B = 2$ particle with mass below $2m_\Lambda$ would decay via weak interactions and, thus, be long-lived with a lifetime comparable to that of the Λ and negligible natural width.

Jaffe's specific prediction was ruled out by the observation of double-Λ hypernuclei events [2–4], especially the famous "Nagara" event that has a relatively unambiguous signature as a ${}^{6}_{\Lambda\Lambda}$He hypernucleus produced via Ξ^- capture in emulsion [3]. The measured $\Lambda\Lambda$ binding energy, $B_{\Lambda\Lambda} = 7.13 \pm 0.87$ MeV, establishes, with a 90% confidence level (C.L.), a lower limit of $M_H > 2223.7$ MeV, severely narrowing the window for a stable H to the binding energy range $B_H \equiv 2m_\Lambda - M_H < 7.9$ MeV.

Although Jaffe's original prediction for $B_H \simeq 81$ MeV has been ruled out, the theoretical case for an H dibaryon with a mass near $2m_\Lambda$ continues to be strong and has been recently strengthened by lattice QCD calculations (LQCD) by the NPLQCD [5,6] and HALQCD [7] collaborations that both find a bound H dibaryon, albeit for nonphysical values for the pion mass. NPLQCD's linear (quadratic) extrapolation to the physical pion mass gives $B_H = -0.2 \pm 8.0$ MeV (7.4 ± 6.2 MeV) [6]. Carames and Valcarce [8] recently studied the H with a chiral constituent model constrained by ΛN, ΣN, ΞN and $\Lambda\Lambda$ cross section data and find B_H values that are similar to the NPLQCD extrapolated values.

These recent theoretical results motivate searches for the H with mass near the $M_H = 2m_\Lambda$ threshold. For masses approaching the $2m_\Lambda$ threshold from below (above), the H would behave more and more like a $\Lambda\Lambda$ analog of the deuteron (dineutron), independently of its dynamical origin [9]. If its mass is below $2m_\Lambda$, the H would predominantly decay via $\Delta S = +1$ weak transitions to Λn, $\Sigma^- p$, $\Sigma^0 n$ or $\Lambda p\pi^-$ final states. If its mass is above $2m_\Lambda$, but below $m_{\Xi^0} + m_n (= 2m_\Lambda + 23.1$ MeV), the H would decay via strong interactions to $\Lambda\Lambda$ 100% of the time.

The E522 collaboration at KEK studied $\Lambda\Lambda$ production in the ${}^{12}\mathrm{C}(K^-, K^+\Lambda\Lambda X)$ reaction and reported an

intriguing near-threshold enhancement but with limited statistics [10]. The BNL-E836 Collaboration searched for the $\Delta S = +2$ reaction $^3\mathrm{He}(K^-, K^+)Hn$ and established cross section limits spanning the range 50 MeV $\leq B_H \leq$ 380 MeV [11]. Searches for a bound H decaying to $\Lambda p\pi^-$ reported negative results [12,13]. Earlier searches, also with negative results, are listed in Ref. [14].

Decays of narrow $\Upsilon(nS)$ $(n = 1, 2, 3)$ bottomonium $(b\bar{b})$ resonances are particularly well suited for searches for multiquark states with nonzero strangeness. The $\Upsilon(nS)$ states are flavor-$SU(3)$ singlets and primarily decay via the three-gluon annihilation process (e.g., $(\mathcal{B}(\Upsilon(1S) \to ggg) = 81.7 \pm 0.7\%$ [15]). The gluons materialize into $u\bar{u}$, $d\bar{d}$ and $s\bar{s}$ pairs in roughly equal numbers. The high density of quarks and antiquarks in the limited final-state phase space is conducive to the production of multi-quark systems, as demonstrated by large branching fractions for inclusive antideuteron $(\bar{d})$ production: $\mathcal{B}(\Upsilon(1S) \to \bar{d}X) = (2.9 \pm 0.3) \times 10^{-5}$ and $\mathcal{B}(\Upsilon(2S) \to \bar{d}X) = (3.4 \pm 0.6) \times 10^{-5}$ [16]. An upper limit for the production of a six-quark $S = -2$ state in $\Upsilon(nS)$ decays that is substantially below that for the six-quark antideuteron would be strong evidence against its existence.

Here we report results of a search for H dibaryon production in the inclusive processes $\Upsilon(1S, 2S) \to HX$, $H \to \Lambda p\pi^-$ and $\Lambda\Lambda$ [17]. We use data samples containing 102 million $\Upsilon(1S)$ and 158 million $\Upsilon(2S)$ decays collected with the Belle detector operating at the KEKB e^+e^- collider [18]. The data were accumulated at center-of-mass system (c.m.s.) energies of $\sqrt{s} = 9.460$ GeV and 10.023 GeV, which correspond to the $\Upsilon(1S)$ and $\Upsilon(2S)$ resonance peaks, respectively. Contributions from the $e^+e^- \to q\bar{q}$ ($q = u, d, s$, and c) continuum process are inferred from a 63.7 fb^{-1} sample collected at $\sqrt{s} = 10.53$ GeV and scaled by luminosity and $1/s$. We assume equal $\Upsilon(1S)$ and $\Upsilon(2S)$ branching fractions, i.e., $\mathcal{B}(\Upsilon(1S) \to HX) = \mathcal{B}(\Upsilon(2S) \to HX) \equiv \mathcal{B}(\Upsilon(1S, 2S) \to HX)$.

Belle is a large-solid-angle magnetic spectrometer consisting of a silicon vertex detector, a cylindrical drift chamber (CDC), an array of aerogel threshold Cherenkov counters, a barrel-like arrangement of time-of-flight scintillation counters, and an electromagnetic calorimeter comprised of CsI(Tl) crystals located inside a superconducting solenoid coil that provides a 1.5 T magnetic field. Measurements of dE/dx in the CDC, aerogel threshold Cherenkov counters light yields, time-of-flight times and electromagnetic calorimeter energy deposits are combined to form particle identification (pid) likelihoods $\mathcal{L}(h)$ ($h = e^+$, π^+, K^+ or p) for charged tracks. The $\mathcal{R}(h|h') = \mathcal{L}(h)/(\mathcal{L}(h) + \mathcal{L}(h'))$ ratios are used to make pid assignments. Belle is described in detail elsewhere [19].

Samples of simulated $\Upsilon(1S)$ and $\Upsilon(2S)$ Monte Carlo (MC) events, generated with PYTHIA [20] and simulated using GEANT3 [21], are used to study backgrounds and determine efficiencies. For signal MC events for various H decay modes, we use PYTHIA with the $\Xi(1530)^0$ mass, width and decay-table entries replaced with hypothesized parameters for the H. For MC-based optimization of selection criteria, we optimize a figure of merit defined as $FoM = n_{\mathrm{sig}}/\sqrt{n_{\mathrm{sig}} + n_{\mathrm{bkg}}}$, where n_{sig} (n_{bkg}) is the number of selected signal (background) events assuming $\mathcal{B}(\Upsilon(nS) \to HX) = 3 \times 10^{-5}$.

For both investigated channels, event selection starts with the identification of a Λ candidate reconstructed via its $p\pi^-$ decay using the Λ-momentum-dependent criteria based on proton pid, track vertex information, decay length, and $M(p\pi^-)$ described in Ref. [22]. The $M(p\pi^-)$ distribution for selected candidates is well fitted by a Lorentzian function with a FWHM resolution for the Λ peak of 1.50 ± 0.01 MeV. For Λ candidates, we require $\Delta M_\Lambda \equiv |M(p\pi) - m_\Lambda| < 3.0$ MeV.

For the $H \to \Lambda p\pi^-$ search, the $p\pi^-$ track selection requirements are optimized using FoMs determined by MC calculations assuming $\tau_H = \tau_\Lambda$. Both the p and π^- are required to be well identified by the pid measurements $\mathcal{R}(p|h^+) > 0.9$ $(h^+ = \pi^+$ or $K^+)$ $\mathcal{R}(\pi^-|e^-) > 0.9$ and $\mathcal{R}(\pi^-|K^-) > 0.6$ [23]. We require that the p and π^- tracks and the Λ trajectory satisfy a fit to a common vertex. In addition we require $c\tau_{\Lambda p\pi^-} \geq 0.0$, where $c\tau \equiv \vec{\ell} \cdot \vec{p}_H M_H/|\vec{p}_H|^2$ and $\vec{\ell}$ is the displacement between the run-dependent average interaction point (IP) and the fitted vertex position. In some cases, the tracking algorithm finds two reconstructed tracks with nearly the same parameters from CDC hits produced by a single particle. Contamination from this source is removed by the requirements $M(p_1p_2) \geq 1878$ MeV, $M(\pi_1^-\pi_2^-) \geq 280$ MeV and $N_{\mathrm{hits}}(p_1) + N_{\mathrm{hits}}(p_2) \geq 50$, where $H \to \Lambda p_2\pi_2^-$; $\Lambda \to p_1\pi_1^-$ and $N_{\mathrm{hits}}(p_i)$ is the number of CDC hits used to reconstruct the ith proton. In the $\Lambda p\pi^-$ mode, there is a large background from Λ and p production via secondary interactions in the material of the beam pipe and inner detector. This is removed by requiring $|\vec{p}_h| > 0.5$ GeV for both $h = \Lambda$ and $h = p$; this requirement is not applied to the $\bar{\Lambda}\,\bar{p}\,\pi^+$ channel. In 6.3% (5.2%) of the data (MC) events, there are two or more entries that have one or more tracks in common. In these cases, the combination with the smallest χ^2 value from the $\Lambda p\pi^-$ common vertex fit is selected. For signal MC events, this chooses the correct combination 93.4% of the time. The $\Lambda \to p_1\pi_1^-$ candidate is subjected to a kinematic fit that constrains $M(p_1\pi_1^-)$ to m_Λ. The final selection efficiencies are determined from MC by averaging $\Upsilon(1S)$ and $\Upsilon(2S)$ signal MC to be $\epsilon_1 = 7.7\%$ for $H \to \Lambda p\pi^-$ and $\bar{\epsilon}_1 = 8.8\%$ for $\bar{H} \to \bar{\Lambda}\,\bar{p}\,\pi^+$.

The resulting continuum-subtracted $M(\Lambda p\pi^-)$ $(M(\bar{\Lambda}\,\bar{p}\,\pi^+))$ distribution for the combined $\Upsilon(1S)$ and $\Upsilon(2S)$ samples, shown in the top (bottom) panel of Fig. 1, has no evident $H \to \Lambda p\pi^-$ $(\bar{H} \to \bar{\Lambda}\,\bar{p}\,\pi^+)$ signal. The curve in the figure is the result of a fit using an ARGUS-like threshold function to model the background

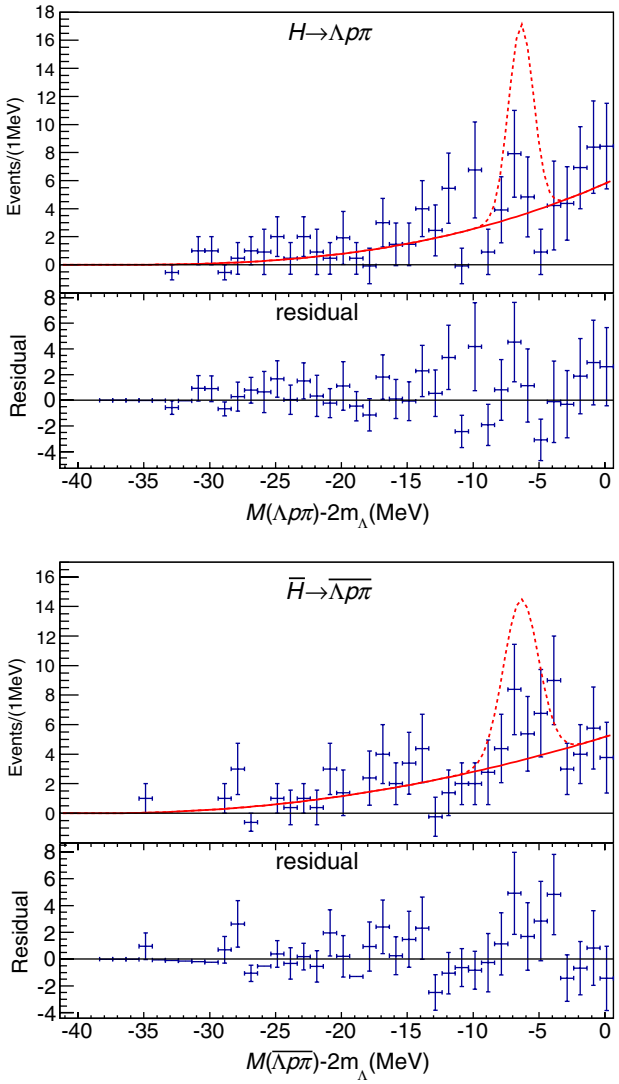

FIG. 1 (color online). *Top*: The continuum-subtracted $M(\Lambda p\pi^-)$ distribution (upper) and fit residuals (lower) for the combined $\Upsilon(1S)$ and $\Upsilon(2S)$ data samples. The curve shows the results of the background-only fit described in the text. The dashed curve shows the expected H signal for a $\Upsilon(1S,2S)\to HX$ branching fraction that is 1/20th that for antideuterons. *Bottom*: The corresponding $M(\bar\Lambda\,\bar p\,\pi^+)$ distributions.

[24]; fit residuals are also shown. The dashed curve in the figure shows the expected H signal for a $\Upsilon(1S, 2S) \to HX$ branching fraction that is 1/20th that for antideuterons.

For the second Λ (Λ_2) in the $H \to \Lambda_1\Lambda_2$ ($\Lambda_i \to p_i\pi_i^-$) channel, in addition to the criteria used for Λ_1 selection, FoMs based on MC events are used to optimize additional requirements on a fit that constrains the $\Lambda_1\Lambda_2$ vertex to the IP, and $c\tau_{\Lambda_2} \geq -0.5$ cm. Entries in which two of the selected tracks originate from a single particle are removed by the requirements $M(p_1p_2) \geq 1878$ MeV, $M(\pi_1^-\pi_2^-) \geq 288$ MeV and $N_{\rm hits}(p_1) + N_{\rm hits}(p_2) \geq 60$. In 3.2% (2.8%) of the data (MC) events, two or more entries have one or more tracks in common. In these cases, we choose the track combination that has the best $\Lambda\Lambda$-IP vertex fit. For signal MC events, this selects the correct combination 95.4% of the time. The $\Lambda\Lambda$ candidates are subjected to a kinematic fit that constrains both $p\pi^-$ masses to m_Λ. The MC-determined selection efficiencies, obtained by averaging $\Upsilon(1S)$ and $\Upsilon(2S)$ signal MC results, are $\epsilon_2 = 10.9\%$ for $H \to \Lambda\Lambda$ and $\bar\epsilon_2 = 10.1\%$ for $\bar H \to \bar\Lambda\bar\Lambda$.

The difference between the $\Lambda\Lambda$ and $\bar\Lambda\bar\Lambda$ signal yields in the region $M(\Lambda\Lambda) < 2.38$ GeV, determined from two-dimensional fits to scatter plots of $M(p_1\pi_1)$ vs $M(p_2\pi_2)$ with the Λ mass requirements relaxed, is larger than the difference in the MC-determined $\Lambda\Lambda$ and $\bar\Lambda\bar\Lambda$ acceptances. This is attributed to deficiencies in the simulation of low-energy $\bar\Lambda$ and $\bar p$ inelastic interactions in the material of the inner detector. To account for this, a correction factor of 0.83 ± 0.13 is applied to the $H \to \bar\Lambda\bar\Lambda$ and $H \to \bar\Lambda\,\bar p\,\pi^+$ efficiencies. The error on this factor is included in the systematic error.

The continuum-subtracted $M(\Lambda\Lambda)$ ($M(\bar\Lambda\bar\Lambda)$) distribution for events that satisfy all of the selection requirements is shown in the top (bottom) panel of Fig. 2, where there is no sign of a near-threshold enhancement similar to that reported by the E522 Collaboration [10] nor any other evident signal for $H \to \Lambda\Lambda$ ($\bar H \to \bar\Lambda\bar\Lambda$). The curve is the result of a background-only fit using the functional form described above; fit residuals are also shown. Expectations for a signal branching fraction that is 1/20 that for the antideuterons is indicated with a dashed curve.

For each channel, we do a sequence of binned, minimum χ^2 fits to the invariant mass distributions in Figs. 1 and 2 using a signal function to represent $H \to f_i$ ($f_1 = \Lambda p\pi^-$ and $f_2 = \Lambda\Lambda$) and an ARGUS function to represent the background. In the fits, the signal peak position is confined to a 4 MeV window that is scanned in 4 MeV steps across the ranges $(m_\Lambda + m_p + m_{\pi^-}) \leq M(\Lambda p\pi^-) \leq 2m_\Lambda$ and $2m_\Lambda \leq M(\Lambda\Lambda) \leq 2m_\Lambda + 28$ MeV. For the $\Lambda p\pi^-$ ($\bar\Lambda\,\bar p\,\pi^+$) mode, the signal function is a Gaussian whose resolution width is fixed at its MC-determined value scaled by a factor $f = 0.85(1.12)$ that is determined from a comparison of data and MC fits to inclusive $\Xi^- \to \Lambda\pi^-$ and $\Xi_c(2470)^0 \to \Xi^-\pi^+$ signals found in the same data samples. For the $\Lambda\Lambda$ mode, the signal function is a Lorentzian with FWHM fixed at either $\Gamma = 0$ or 10 MeV convolved with a Gaussian. Since the f_i and $\bar f_i$ acceptances are different, we fit the particle and antiparticle distributions separately.

None of the fits exhibit a positive signal with greater than 3σ significance. The fit results are translated into 90% C.L. upper limits on the signal yield, $N_i^{\rm UL}(M_H)$ and $\bar N_i^{\rm UL}(M_H)$, by convolving a normalized function of the form $\exp(-\Delta\chi^2/2)$ with a normalized Gaussian whose width equals the systematic error (discussed below) and then determining the yield below which 90% of the area above $N_i = 0$ is contained. These values are used to determine upper limits on the inclusive product branching fractions via the relation

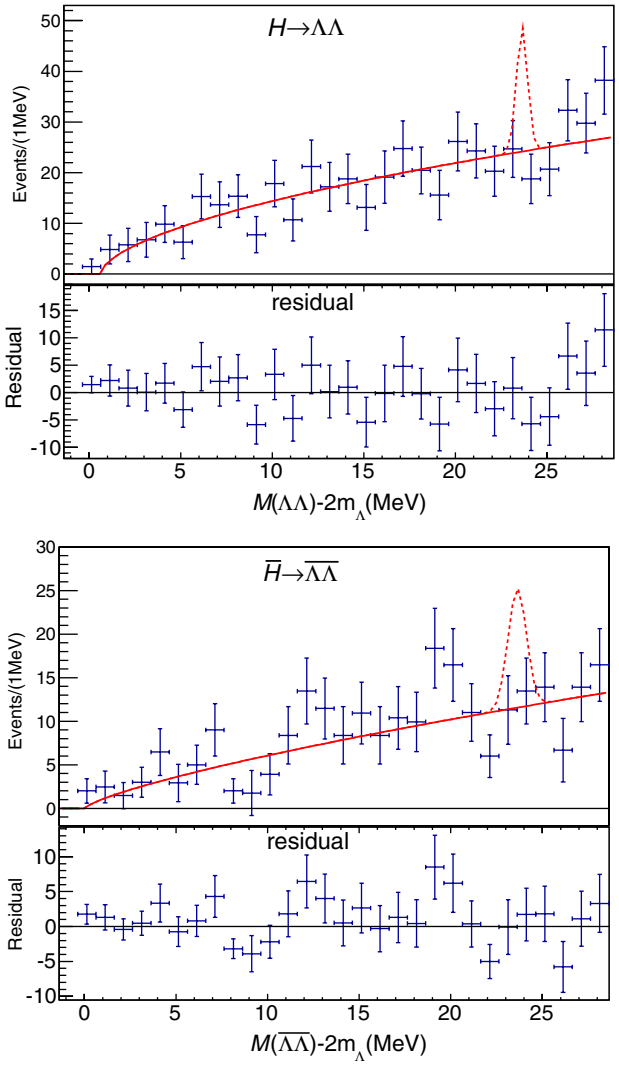

FIG. 2 (color online). *Top*: The continuum-subtracted $M(\Lambda\Lambda)$ distribution (upper) and fit residuals (lower) for the combined $\Upsilon(1S)$ and $\Upsilon(2S)$ data samples with the background-only fit superimposed. The curves are the same as in Fig. 1. *Bottom*: The corresponding $M(\bar{\Lambda}\,\bar{\Lambda})$ distributions.

$$\mathcal{B}(\Upsilon(1S, 2S) \to HX)\mathcal{B}(H \to f_i) < \frac{1}{2N_\Upsilon(\mathcal{B}_{\Lambda\to p\pi^-})^i}\frac{N_i^{\rm UL}(M_H)}{\epsilon_i}, \quad (1)$$

where $N_\Upsilon = (260 \pm 6) \times 10^6$ is the total number of $\Upsilon(1S)$ plus $\Upsilon(2S)$ events in the data sample [25] and $\mathcal{B}_{\Lambda\to p\pi^-} = 0.639 \pm 0.005$ [15].

Sources of systematic errors and their contributions are listed in Table I. The tracking, pid, and Λ reconstruction uncertainties are common to other Belle analyses and are determined from data-MC comparisons of various control samples. For the channel-specific vertex requirements, we use data-MC differences found in high-statistics samples of inclusive $\Upsilon(1S, 2S) \to \Lambda\bar{p}\pi^+$ and $\Lambda\bar{\Lambda}$ events with $M(\Lambda\bar{p}\pi) < 2.28$ GeV ($M(\Lambda\bar{\Lambda}) < 2.38$ GeV) selected with the same vertex criteria. The continuum subtraction

TABLE I. Systematic error sources (in percent). When the H and $\bar{H}$ values differ, the $\bar{H}$ values are given in parentheses.

Source	$H \to \Lambda p\pi^-$	$H \to \Lambda\Lambda$
$N_{\Upsilon(1S)} + N_{\Upsilon(2S)}$	2.3	2.3
Tracking	3.6	3.6
Particle id	7.2	4.3
Λ reconstruction	3.2(5.3)	12.6(9.6)
Vertex requirements	3.9	3.5
Signal efficiency	2.0(15.7)	1.9(15.8)
Continuum subtraction	1.4	1.4
$\mathcal{B}(\Lambda \to p\pi^-)$	0.8	1.6
PDG Fitting	2.0	2.0
Resolution	2.6	2.6
Quadrature sum	10.2(19.1)	14.7(19.8)

systematic error contribution is determined from the errors in the relative on- and off-resonance luminosity measurements. Systematic errors associated with the MC-determined acceptance and minimum momentum requirement are determined by varying parameters used in the PYTHIA generator and GEANT simulation programs. The systematic errors associated with the signal fitting are determined from changes induced by variations in the binning and fitting ranges in fits to an inclusive $\Xi_c(2470)^0 \to \Xi^-\pi^+$ signal seen in the same data sample. Sums in quadrature of the individual contributions are taken as the total systematic errors.

For the final limits, we use the branching fraction value that contains <90% of the above-zero area of the product of the H and $\bar{H}$ likelihood functions. Figure 3 shows the resulting $M_H - 2m_\Lambda$-dependent upper limits for the $\Lambda p\pi^-$

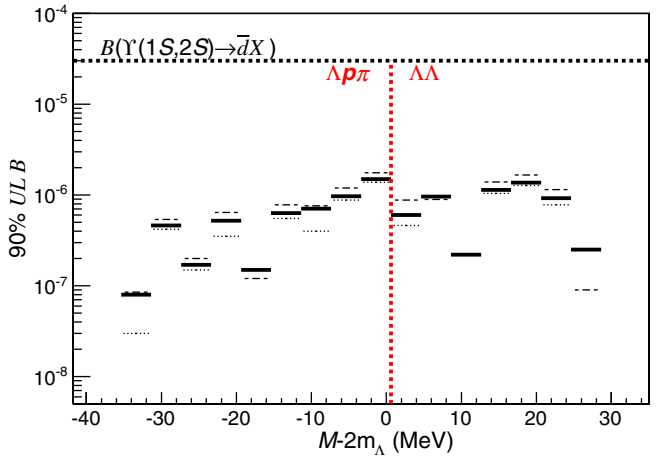

FIG. 3 (color online). Upper limits (at 90% C.L.) for $\mathcal{B}(\Upsilon(1S, 2S) \to HX)$ for a narrow ($\Gamma = 0$) H dibaryon vs $M_H - 2m_\Lambda$ are shown as solid horizontal bars. The $+1\sigma$ ($+2\sigma$) values from the fitted signal yields are shown as the dotted (dashed) bars. (For some mass bins, these are negative and not shown.) The vertical dotted line indicates the $M_H = 2m_\Lambda$ threshold. The limits below (above) the $2m_\Lambda$ threshold are for $f_1 = \Lambda p\pi^-$ ($f_2 = \Lambda\Lambda$). The horizontal dotted line indicates the average PDG value for $\mathcal{B}(\Upsilon(1S, 2S) \to \bar{d}X)$.

TABLE II. 90% C.L. upper limits ($\times 10^{-7}$) on the product branching fraction $\mathcal{B}(\Upsilon(1S, 2S) \to HX)\mathcal{B}(H \to f_i)$, $f_1 = \Lambda p\pi^-$; $\delta M_1 = 2m_\Lambda - M_H$ and $f_2 = \Lambda\Lambda$; $\delta M_2 = M_H - 2m_\Lambda$.

δM_i (MeV)	2	6	10	14	18	22	26	30	34
$f_1 = \Lambda p\pi^-$	15.	9.7	7.1	6.3	1.5	5.2	1.7	4.6	0.8
$f_2 = \Lambda\Lambda$									
$\Gamma = 0$	6.0	9.6	2.2	11.	14.	9.2	2.5		
$\Gamma = 10$ MeV	16.	17.	15.	37.	44.	42.	33.		

and $\Lambda\Lambda$ (for $\Gamma = 0$) modes. The upper limit values, listed in Table II, are all more than an order of magnitude lower than the average of measured values of $\mathcal{B}(\Upsilon(1S, 2S) \to \bar{d}X)$, shown in Fig. 3 as a horizontal dotted line.

The $H \to \Lambda p\pi^-$ limits quoted in Table II and shown in Fig. 3 are determined for an H lifetime $\tau_H = 0.263$ ns, i.e., the Λ lifetime. The acceptance decreases and, therefore, the limits increase, with increasing lifetime: for $\tau_H = 5\tau_\Lambda$, the acceptance is a factor of two lower and the limits are correspondingly twice as high. Conversely, for shorter lifetimes, the acceptance increases: for $\tau = 0.5\tau_\Lambda$, the acceptance is higher and the limits are more stringent by $12 \pm 2\%$.

The results reported here are some of the most stringent constraints to date on the existence of an H dibaryon with mass near the $2m_\Lambda$ threshold [26]. These upper limits are between one and two orders of magnitude below the average of the PDG value for inclusive $\Upsilon(1S)$ and $\Upsilon(2S)$ decays to antideuterons. Since $\Upsilon \to$ hadrons decays produce final states that are flavor-$SU(3)$ symmetric, this suggests that if an H dibaryon exists in this mass range, it must have very different dynamical properties than the deuteron, or, in the case of $M_H < 2m_\Lambda$, a strongly suppressed $H \to \Lambda p\pi^-$ decay mode.

We thank the KEKB group for excellent operation of the accelerator; the KEK cryogenics group for efficient solenoid operations; and the KEK computer group, the NII, and PNNL/EMSL for valuable computing and SINET4 network support. We acknowledge support from MEXT, JSPS and Nagoya's TLPRC (Japan); ARC and DIISR (Australia); NSFC (China); MSMT (Czechia); DST (India); INFN (Italy); MEST, NRF, GSDC of KISTI, and WCU (Korea); MNiSW (Poland); MES and RFAAE (Russia); ARRS (Slovenia); SNSF (Switzerland); NSC and MOE (Taiwan); and DOE and NSF (USA). B.-H. Kim and S. L. Olsen acknowledge support from NRF (Korea) Grant No. 2011-0029457 and WCU Grant No. R32-10155.

[1] R. L. Jaffe, Phys. Rev. Lett. **38**, 195 (1977).
[2] M. Danysz, K. Garbowska, J. Pniewski, and J. Zakrzewski, Phys. Rev. Lett. **11**, 29 (1963); D. J. Prowse, Phys. Rev. Lett. **17**, 782 (1966); S. Aoki *et al.*, Prog. Theor. Phys. **85**, 1287 (1991).
[3] H. Takahashi *et al.*, Phys. Rev. Lett. **87**, 212502 (2001).
[4] K. Nakazawa *et al.* (E176 Collaboration), Nucl. Phys. **A835**, 207 (2010).
[5] S. R. Beane *et al.* (NPLQCD Collaboration), Phys. Rev. Lett. **106**, 162001 (2011).
[6] S. R. Beane *et al.* (NPLQCD Collaboration), Mod. Phys. Lett. A **26**, 2587 (2011).
[7] T. Inoue, N. Ishii, S. Aoki, T. Doi, T. Hatsuda, Y. Ikeda, K. Murano, H. Nemura, and K. Sasaki (HALQCD Collaboration), Phys. Rev. Lett. **106**, 162002 (2011).
[8] S. R. Carames and A. Valcarce, Phys. Rev. C **85**, 045202 (2012).
[9] E. Braaten (private communication); See also, E. Braaten and H.-W. Hammer, Phys. Rep. **428**, 259 (2006).
[10] C. J. Yoon *et al.* (KEK-PS E522 Collaboration), Phys. Rev. C **75**, 022201(R) (2007); See also J. K. Ahn *et al.* (KEK-PS E224 Collaboration), Phys. Lett. B **444**, 267 (1998); J. Belz *et al.* (BNL E888 Collaboration), Phys. Rev. D **53**, R3487 (1996).
[11] R. W. Stotzer *et al.* (BNL-E836 Collaboration), Phys. Rev. Lett. **78**, 3646 (1997).
[12] A. Alavi-Harati *et al.* (KTeV Collaboration), Phys. Rev. Lett. **84**, 2593 (2000).
[13] I. Chemakin *et al.* (E910 Collaboration), Nucl. Phys. **A639**, 407c (1998).
[14] J. K. Ahn *et al.* (KEK-PS E224 Collaboration), Phys. Lett. B **444**, 267 (1998); , J. Belz *et al.*, Phys. Rev. Lett. **76**, 3277 (1996); J. Belz *et al.*, Phys. Rev. C **56**, 1164 (1997).
[15] J. Beringer *et al.* (Particle Data Group), Phys. Rev. D **86**, 010001 (2012).
[16] D. M. Asner *et al.* (CLEO Collaboration), Phys. Rev. D **75**, 012009 (2007); see also H. Albrecht *et al.* (ARGUS Collaboration), Phys. Lett. B **236**, 102 (1990).
[17] The inclusion of charge-conjugate modes is implied unless explicitly stated otherwise.
[18] S. Kurokawa and E. Kikutani, Nucl. Instrum. Methods Phys. Res., Sect. A **499**, 1 (2003), and other papers included in this volume.
[19] A. Abashian *et al.* (Belle Collaboration), Nucl. Instrum. Methods Phys. Res., Sect. A **479**, 117 (2002); Y. Ushiroda (Belle SVD2 Group), Nucl. Instrum. Methods Phys. Res., Sect. A **511**, 6 (2003).
[20] T. Sjöstrand, S. Mrenna, and P. Skands, J. High Energy Phys. 05 (2006) 026.
[21] R. Brun *et al.*, GEANT 3.21, CERN Report DD/EE/84-1, 1984.
[22] K. Abe *et al.* (Belle Collaboration), Phys. Rev. D **65**, 091103 (2002).
[23] These pid requirements correspond to a p (π) efficiency of 86% (93%) and $h \to p$ ($K \to \pi$) misidentification probability less than 1% (7.5%).
[24] H. Albrecht *et al.* (ARGUS Collaboration), Phys. Lett. B **241**, 278 (1990). We use $f(x) = x\sqrt{(x/m_0)^2 - 1} \times \exp[-a((x/m_0)^2 - 1)]$.
[25] X. L. Wang *et al.* (Belle Collaboration), Phys. Rev. D **84**, 071107(R) (2011).
[26] The sample of $\Lambda\Lambda$ plus $\bar{\Lambda}\bar{\Lambda}$ events with $M(\Lambda\Lambda)$ below the $m_{\Xi^-} + m_p$ threshold detected in this experiment, as determined from the fits to the two dimensional $M(p_1\pi_1^-)$ vs $M(p_2\pi_2^-)$ histograms described in the text, contains 2.3×10^3 events and is nearly two orders of magnitude larger than the 28 $\Lambda\Lambda$ events with invariant mass below $m_{\Xi^-} + m_p$ used in KEK experiment E522.